

# Flexible resistive random access memory using solution-processed $\text{TiO}_x$ with Al top electrode on Ag layer-inserted indium-zinc-tin-oxide-coated polyethersulfone substrate

Seungjae Jung,<sup>1</sup> Jaemin Kong,<sup>1</sup> Sunghoon Song,<sup>1</sup> Kwanghee Lee,<sup>1,2,3</sup> Takhee Lee,<sup>1,3</sup> Hyunsang Hwang,<sup>1,3,a)</sup> and Sanghun Jeon<sup>4,b)</sup>

<sup>1</sup>*School of Materials Science and Engineering, Gwangju Institute of Science and Technology, Gwangju 500-712, South Korea*

<sup>2</sup>*Heeger Center for Advanced Materials, Gwangju Institute of Science and Technology, Gwangju 500-712, South Korea*

<sup>3</sup>*Department of Nanobio Materials and Electronics, Gwangju Institute of Science and Technology, Gwangju 500-712, South Korea*

<sup>4</sup>*Semiconductor Devices Laboratory, Samsung Advanced Institute of Technology, Yongin-si, Gyeonggi-do 446-712, South Korea*

(Received 28 March 2011; accepted 13 July 2011; published online 5 October 2011)

We demonstrated a flexible resistive random access memory (FRerAM) device using a solution-processed  $\text{TiO}_x$  active layer with an Al top electrode on an Ag layer-inserted indium-zinc-tin-oxide (IAI)-coated polyethersulfone substrate (Al/ $\text{TiO}_x$ /IAI). Its feasibility of FRerAM application was evaluated through the comparison of electrical and mechanical characteristics with devices having different structure such as Ag/ $\text{TiO}_x$ /Ag, Al/ $\text{TiO}_x$ /indium-tin-oxide, and Al/ $\text{TiO}_x$ /Al. As a result, our FRerAM device exhibited greater FRerAM performance such as stable memory characteristics under mechanically bent conditions and robustness to repetitive bending cycles. In addition, the device was thermally stable up to 85 °C, despite its flexible electrode and polymer substrate. © 2011 American Institute of Physics. [doi:10.1063/1.3621826]

Recently, several mechanically flexible devices have been intensively investigated for various future electronic device applications.<sup>1–12</sup> Among them, the flexible ReRAM (FRerAM) device has been considered as a promising candidate for the memory component of flexible electronic circuits.<sup>1,2,7–12</sup> According to these previous reports, it is evident that FRerAM performance is determined by the stability of the electrical and mechanical properties of each layer comprising the memory device under structurally bent, thermal, and electrical operation conditions. Further, the FRerAM performance is also dependent on process compatibility to the flexible polymer substrate.

In this study, we fabricated a reliable FRerAM device using an Al top electrode, a solution-processed  $\text{TiO}_x$  active layer, and an Ag layer-inserted indium-zinc-tin-oxide (IAI)-coated polyethersulfone (PES) substrate and evaluated its feasibility of FRerAM application through the comparison of electrical and mechanical characteristics with devices incorporated with various electrodes such as Ag, indium-tin-oxide (ITO), and Al, which are already reported as flexible electrodes of ReRAM device in the previous studies.<sup>1,7–11</sup>

The IAI-coated PES substrate was prepared by the insertion of 14-nm-thick Ag layer between sputtered 30-nm-thick top and bottom indium-zinc-tin-oxide films on PES substrate. For comparison, 80-nm-thick Ag, ITO, and Al films were also deposited on PES substrates as bottom electrodes (BEs), using e-beam evaporation.

Starting solution for the fabrication of solution-processed  $\text{TiO}_x$  active layer was prepared by the mixture of

titanium(IV) isopropoxide ( $\text{Ti}[\text{OCH}(\text{CH}_3)_2]_4$ ) precursor, 2-methoxyethanol ( $\text{CH}_3\text{OCH}_2\text{CH}_2\text{OH}$ ), and ethanolamine ( $\text{H}_2\text{NCH}_2\text{CH}_2\text{OH}$ ). The detailed procedure is described in our previous report.<sup>13</sup> In order to fabricate FRerAM devices, spin-coating was performed on PES substrates coated with four different BEs using the prepared  $\text{TiO}_x$  solution. Subsequently, the substrates were made to undergo a hydrolysis reaction for 1 h in ambient air. The thickness of the fabricated  $\text{TiO}_x$  film was approximately 50 nm. Finally, an Ag or Al top electrode with a diameter of 50  $\mu\text{m}$  was formed by an e-beam evaporator using a shadow mask. For the elimination of solvent and precursors and the improvement of interfacial quality between  $\text{TiO}_x$  and electrodes, the fabricated device was post-annealed at 150 °C in ambient  $\text{N}_2$  for 10 min. Finally, we fabricated FRerAM devices with four different structures such as Ag/ $\text{TiO}_x$ /Ag, Al/ $\text{TiO}_x$ /ITO, Al/ $\text{TiO}_x$ /Al, and Al/ $\text{TiO}_x$ /IAI (denoted as the “Ag device,” “ITO device,” “Al device,” and “IAI device”).

First of all, in order to choose a suitable bent condition for electrical characterization, each of the 20 devices was investigated under various degrees of structural bending conditions using the current-voltage (I-V) measurements (Fig. 1). As described in the left inset in Fig. 1(a), the bending condition is represented by the distance between the two end points of the bending arc (denoted as “ $d = X \text{ mm}$ ”). Interestingly, initial state of the Ag device was not resistive at all, and separated memory states never appeared. Considering a previous report in which  $\text{TiO}_2$  layer formed by atomic layer deposition is used as an electrolyte of Cu diffusion,<sup>14</sup> Ag diffusion into relatively porous solution-processed  $\text{TiO}_x$  layer during post-annealing process at 150 °C can be a plausible origin of this behavior. On the contrary, the ITO, Al, and IAI

<sup>a)</sup>Electronic mail: hwanghs@gist.ac.kr.

<sup>b)</sup>Electronic mail: sanghun1.jeon@samsung.com.

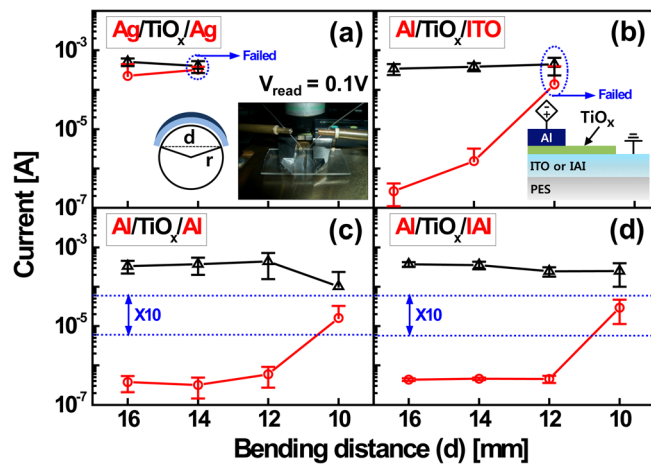


FIG. 1. (Color online) Current level of two resistance states for (a) the Ag, (b) ITO, (c) Al, and (d) IAI devices as a function of bending distance in the range from 16 mm to 10 mm. Bending radius ( $r$ ) and distance ( $d$ ) are described in the left inset of (a). Right inset of (a) and the inset of (b) show picture for current level measurement of bent device and the illustration of a fabricated device structure, respectively.

devices exhibited a reversible resistive switching with less than 10% failure up to bending radii of 14, 12, and 12 mm, respectively. Therefore, the bending tests were conducted under the bending condition of  $d = 12$  mm and the Ag device was excluded from all next measurements.

Figure 2(a) exhibits the comparison of the typical I-V curves of the FReRAM devices. All devices show typical bipolar switching behavior under the compliance current of 1 mA of the control circuit. While the Al and IAI devices exhibited almost identical switching characteristics under flat and bent conditions, only ITO device showed appreciably lower  $V_{\text{set}}$  and  $V_{\text{reset}}$  under bent condition. Such phenomenon was more precisely observed in statistical data measured from 50 switching devices (Fig. 2(b)). Overall, ITO device was switched at lower  $V_{\text{set}}$  and  $V_{\text{reset}}$  and more fluctuant under bent condition, thereby indicating that the Al and IAI devices are more resilient to bending than the ITO device. Contrary to other BEs, distinct cracks were observed in ITO BE by optical microscope.<sup>7,15</sup> Since adhesion

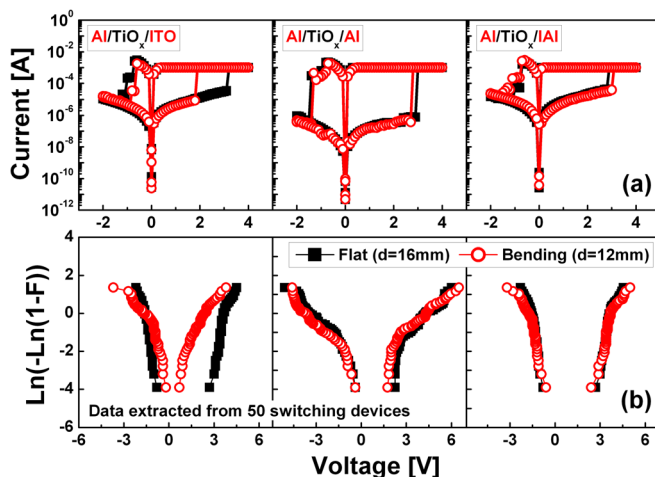


FIG. 2. (Color online) (a) Typical I-V curves and (b) Weibull plots of the  $V_{\text{set}}$  and  $V_{\text{reset}}$  estimated with uniformity tests on 50 switching devices of the ITO, Al, and IAI devices before and under bent conditions.

between  $\text{TiO}_x$  active layer and ITO BE was enhanced by post annealing, the cracks in ITO possibly caused the generation of additional conduction path in the active layer.

Another interesting result is instability of I-V curves and significant fluctuation of  $V_{\text{set}}$  and  $V_{\text{reset}}$  observed in the Al device. Almost identical switching behavior of the Al device before and under bent conditions validates its great flexibility, whereas FReRAM application can be hampered by poor memory characteristics such as unstable switching behavior and non-uniformity of operation voltages. On the other hand, the IAI device is confirmed to satisfy both the requirements.

In order to figure out the origin of different memory properties between the Al and IAI devices, we proposed a simple physical model for switching mechanism, as described in Fig. 3(a). Since Al has stronger tendency to oxidize than Ti,  $\text{AlO}_x$  can be easily formed at Al/ $\text{TiO}_x$  interface during deposition and post-annealing process. This oxidation absorbs oxygen from  $\text{TiO}_x$  layer and then more oxygen-deficient  $\text{TiO}_x$  layer is formed at interface. Using X-ray photoelectron spectroscopy (XPS) analysis, we proved the existence of more oxygen-deficient  $\text{TiO}_x$  layers than bulk layers at both the top and bottom interfaces in the Al device, as seen in Fig 3(b). In our previous report on ReRAM device with Al/ $\text{TiO}_x$ /ITO structure, we already found that  $\text{AlO}_x$  interface plays the critical role in forming and subsequent switching processes.<sup>13</sup> Similarly, IAI device exhibited forming and subsequent switching behavior by positive bias application. In contrast, we observed bias polarity independence of these processes in the Al device. Therefore, contrary to the switching behavior of the IAI device caused by the formation/rupture of filament occurred at only top Al/ $\text{TiO}_x$  interface, the switching characteristics of the Al device can be more fluctuant due to enhanced uncontrollability from two interfacial layers. Moreover, considering that the

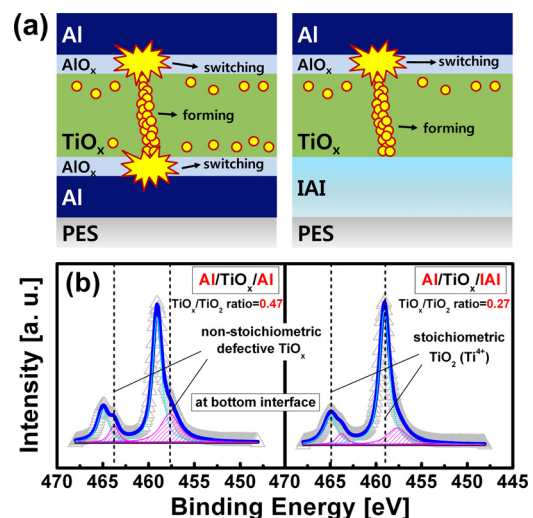


FIG. 3. (Color online) (a) Proposed simple physical model for switching mechanism of the Al and IAI devices. Illustration describes the existence of interfacial layers and the oxygen-deficient layers resulting from the absorption of oxygen atoms by Al electrodes. (b) Ti 2p portions of the XPS spectra of the Al and IAI devices measured "at each  $\text{TiO}_x$ /BE interface."  $\text{TiO}_x/\text{TiO}_2$  ratio of the Al device (0.47), which is similar with that measured in  $\text{TiO}_x/\text{TE}$  interfaces of both the devices, was much higher than that of the IAI device (0.27), which is similar with that measured in  $\text{TiO}_x$  bulks of both the devices.

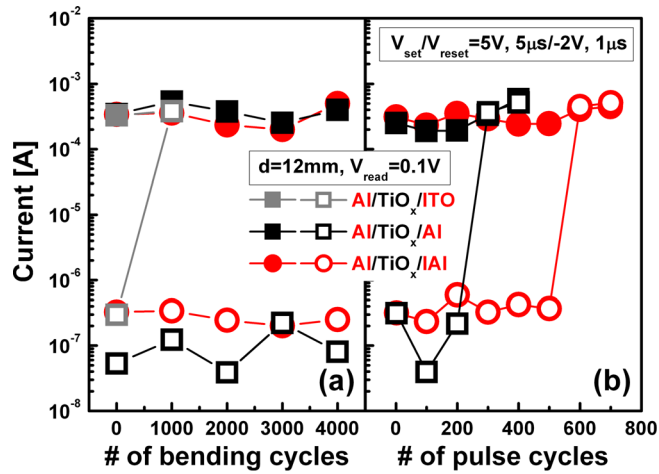


FIG. 4. (Color online) (a) Current level of two resistance states as a function of the number of bending cycles for the ITO, Al, and IAI devices ( $d = 12$  mm). (b) Cycling endurance characteristics of the Al and IAI devices measured by consecutive voltage pulse ( $V_{\text{set}}/V_{\text{reset}} = +5$  V,  $5 \mu\text{s}/-2$  V,  $1 \mu\text{s}$ ).

filament formation is typically caused by defects in active layer and that the multi-filament formation induces the degradation of uniformity, the non-uniformity of the Al device could be worsened by these excess oxygen vacancies. As a result, the IAI device is expected to be more feasible for FReRAM applications.

The current levels of the two resistance states were measured as a function of bending cycles, as seen in Fig. 4(a). In contrast to non-ductile ITO device, the Al and IAI devices retained its two well-separated resistance states without undergoing any significant electrical degradation during the 4000-cycle test, as expected in Fig. 2(a). For analysis on reliability characteristics of the FReRAM devices, we conducted cycling endurance tests (under bent condition) using consecutive voltage pulses ( $V_{\text{set}}/V_{\text{reset}} = +5$  V,  $5 \mu\text{s}/-2$  V,  $1 \mu\text{s}$ ), as depicted in Fig. 4(b). In the case of the Al device, the two memory states could not be differentiated after the endurance test exceeded 200 times pulse repetitions. Additionally, the Al device exhibited fluctuation in HRS current during both bending and pulse endurance tests. In contrast, the IAI device functioned for up to 500 times pulse repetitions during maintaining stable HRS current.

Finally, retention characteristics (substantially the last critical requirement for FReRAM applications) of the devices were measured for up to  $10^4$  s (Fig. 5). Typically, most of the electronic devices comprising organic-based and/or solution-processed active layers and flexible polymer substrates suffer from thermal instability. Therefore, the retention characteristics of our IAI-based FReRAM device were evaluated at elevated temperatures up to  $150^\circ\text{C}$ . No significant current degradation was observed for temperatures up to  $85^\circ\text{C}$  for  $10^4$  s. However, the IAI device started to lose its resistance state after approximately  $10^3$  s at  $150^\circ\text{C}$ . It is noteworthy that the PES substrate began to deform at this point. The thermal stability of the device can further be increased by replacing the PES substrate with more thermally robust substrates such as polyimide.<sup>16</sup>

We demonstrated the reliable performance of a FReRAM device using an Al top electrode, a solution-processed TiO<sub>x</sub> active layer, and an IAI-coated PES sub-

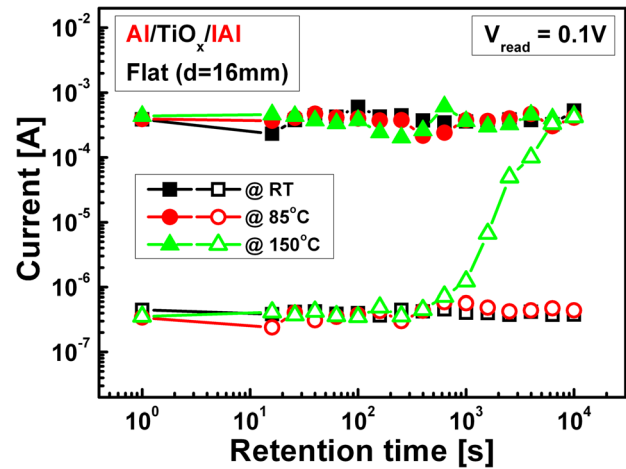


FIG. 5. (Color online) Retention characteristics at various temperature ranges from 25 to  $150^\circ\text{C}$  for the IAI device under mechanically flat condition. Each resistance state was extracted at a reading bias of 0.1 V.

strate. In comparison with the FReRAM device fabricated with various different flexible electrodes, our FReRAM device with Al top and IAI bottom electrodes exhibited superior memory performance and higher level of mechanical flexibility when operated under various test conditions such as varying bending radii, repetitive bending cycles, consecutive voltage pulses, and high-temperature retention characterization. Therefore, we believe that our results will strongly contribute to the development of future electronics based on flexible memory devices.

This work was supported by the National Research Foundation of Korea (NRF) grant funded by the Korea government (MEST) (No. 2011-0018646). K. Lee and J. Kong acknowledge the NRF grant funded by the Korea government (MEST) (No. 2009-0093869).

- <sup>1</sup>N. Gergel-Hackett, B. Hamadani, B. Dunlap, J. Suehle, C. Richter, C. Hacker, and D. Gundlach, *IEEE Electron Device Lett.* **30**, 706 (2009).
- <sup>2</sup>J. Yun, K. Cho, B. Park, B. Park, and S. Kim, *J. Mater. Chem.* **19**, 2082 (2009).
- <sup>3</sup>Y. Ji, B. Cho, S. Song, T. Kim, M. Choe, Y. Kahng, and T. Lee, *Adv. Mater.* **22**, 3071 (2010).
- <sup>4</sup>S. Kim and J. Lee, *Nano Lett.* **10**, 2884 (2010).
- <sup>5</sup>V. Tung, L. Chen, M. Allen, J. Wassei, K. Nelson, R. Kaner, and Y. Yang, *Nano Lett.* **9**, 1949 (2009).
- <sup>6</sup>Q. Cao, H. Kim, N. Pimparkar, J. Kulkarni, C. Wang, M. Shim, K. Roy, M. Alam, and J. Rogers, *Nature* **454**, 495 (2008).
- <sup>7</sup>J. Seo, J. Park, K. Lim, S. Kang, Y. Hong, J. Yang, L. Fang, G. Sung, and H. Kim, *Appl. Phys. Lett.* **95**, 133508 (2009).
- <sup>8</sup>S. Kim and Y. Choi, *Appl. Phys. Lett.* **92**, 223508 (2008).
- <sup>9</sup>S. Kim, H. Moon, D. Gupta, S. Yoo, and Y. Choi, *IEEE Trans. Electron Devices* **56**, 696 (2009).
- <sup>10</sup>H. Jeong, Y. Kim, J. Lee, and S. Choi, *Nanotechnology* **21**, 115203 (2010).
- <sup>11</sup>S. Kim, O. Yarimaga, S. Choi, and Y. Choi, *Solid-State Electron.* **54**, 392 (2010).
- <sup>12</sup>C. Cheng, F. Yeh, and A. Chin, *Adv. Mater.* **23**, 902 (2011).
- <sup>13</sup>S. Jung, J. Kong, S. Song, K. Lee, T. Lee, H. Hwang, and S. Jeon, *J. Electrochem. Soc.* **157**, H1042 (2010).
- <sup>14</sup>L. Yang, C. Kuegeler, K. Szot, A. Ruediger, and R. Waser, *Appl. Phys. Lett.* **95**, 013109 (2009).
- <sup>15</sup>K. Choi, H. Nam, J. Jeong, S. Cho, H. Kim, J. Kang, D. Kim, and W. Cho, *Appl. Phys. Lett.* **92**, 223302 (2008).
- <sup>16</sup>S. Song, B. Cho, T. Kim, Y. Ji, M. Jo, G. Wang, M. Choe, Y. Kahng, H. Hwang, and T. Lee, *Adv. Mater.* **22**, 5048 (2010).